ORIGINAL RESEARCH

Native Coronary Collateral Microcirculation Reserve in Rat Hearts

Xiucheng Liu, MD; Hongyan Dong, PhD; Bing Huang, MSc; Haoran Miao, MSc; Zhiwei Xu, PhD; Yanliang Yuan, PhD; Fan Qiu, PhD; Jiali Chen, MSc; Hao Zhang, MD; Zhiwei Liu, PhD; Xiaoyu Quan, MSc; Lidong Zhu, MSc; Zhongming Zhang, PhD

***Background*—**We occasionally noticed that native collateral blood flow showed a recessive trend in the early stages of acute myocardial infarction in rats, which greatly interferes with the accurate assessment of native collateral circulation levels. Here, we sought to recognize the coronary collateral circulation system in depth, especially the microcirculation part, on this basis.

***Methods and Results*—**In this study, we detected native collateral flow with positron emission tomography perfusion imaging in rats and found that the native flow is relatively abundant when it is initially recruited. However, this flow is extremely unstable in the early stage of acute myocardial infarction and quickly fails. We used tracers to mark the collateral in an ischemic area and a massive preformed collateral network was labeled. The ultrastructures of these collateral microvessels are flawed, which contributes to extensive leakage and consequent interstitial edema in the ischemic region.

***Conclusions*—**An unrecognized short-lived native coronary collateral microcirculation reserve is widely distributed in rat hearts. Recession of collateral blood flow transported by coronary collateral microcirculation reserve contributes to instability of native collateral blood flow in the early stage of acute myocardial infarction. The immature structure determines that these microvessels are short-lived and provide conditions for the development of early interstitial edema in acute myocardial infarction. **(*J Am Heart Assoc*. 2019;8:e011220. DOI: 10.1161/JAHA.118.011220.)**

Key Words: acute myocardial infarction • collateral circulation • coronary microcirculation • edema

Coronary collateral circulation serves as an alternative source of retrograde blood flow for the myocardium to prevent or mitigate acute myocardial infarction (AMI).[1–3] Coronary collateral circulation has been recognized as a significant determinant of severity of myocardial infarction and an important factor affecting mortality in patients with AMI.[4–6] Some analyses also showed that the presence of well-functioning coronary collateral circulation predicted better clinical outcomes independent of myocardial infarct size.[7–9] Its discovery and constant exploration have brought new directions for treatment of ischemic cardiomyopathy.

Coronary collateral circulation is present in humans and other animals regardless of the presence or not of obstructive coronary artery disease.[10,11] Under physiological conditions, there is typically little to no net blood flow in coronary collaterals. Native collaterals serve as a cardiac flow reserve in the absence of occlusion lesions, whereas effective flow is recruited by acute obstruction.[12] In total occlusion lesions, blood flow is completely interrupted, leaving the myocardium entirely dependent on preformed collaterals. Regardless of whether collateral vascular remodeling or compensatory angiogenesis proceeds, they are too time-consuming and cannot be completed in time to save patients.[13,14]

An accurate assessment of the coronary collateral circulation requires a clear distinction between normal antegrade and collateral blood flow. For exclusive characterization of collateral blood flow, coronary occlusion is required, regardless of the method used. Therefore, animal models have been widely used in the study of coronary collateral circulation. However, the time points for assessing native collateral blood flow after acute coronary occlusion have been ambiguous in different studies.[15–17] It is necessary to identify the

From the Department of Thoracic Cardiovascular Surgery, Affiliated Hospital of Xuzhou Medical University, Xuzhou, China (X.L., B.H., H.M., Y.Y., F.Q., J.C., H.Z., X.Q., L.Z., Z.Z.); Morphological Research Experiment Center, Xuzhou Medical University, Xuzhou, China (H.D., Z.L.); Department of Cardiovascular Surgery, Shanghai Chest Hospital, Shanghai Jiaotong University, Shanghai, China (Z.X.).

Correspondence to: Zhongming Zhang, MD, Department of Thoracic Cardiovascular Surgery, Affiliated Hospital of Xuzhou Medical University; Morphological Research Experiment Center, Xuzhou Medical University, 209 Tongshan Road, Jiangsu 221004, China.
E-mail: zhang_zhongming@xzhmu.edu.cn or dhy@xzhmu.edu.cn

Received October 15, 2018; accepted January 22, 2019.

Clinical Perspective

What Is New?

- We introduced an unrecognized short-lived native coronary collateral microcirculation reserve in rat hearts for the first time.
- Recession of anterograde collateral blood flow transported by coronary collateral microcirculation reserve contributes to instability of native collateral blood flow in the early stage of acute myocardial infarction.
- The working mode and structural characteristics of coronary collateral microcirculation reserve present new conjectures for the mechanism of myocardial interstitial edema in the early stage of acute myocardial infarction.

What Are the Clinical Implications?

- Our follow-up study explores further evidence of a similar distribution of coronary collateral microcirculation reserve in humans.
- This study probably gives us a better understanding of the coronary circulatory system and provides a novel countermeasure for management of acute myocardial infarction.

characteristics of native collateral blood flow in the early stage of AMI.

Imaging techniques that measure perfusion are most intuitive and distinctive in collateral assessment, and are widely used in the evaluation of collateral structures and functions in humans and other animals. However, the inherent limitation to collateral assessment with angiography lies in the restricted spatial resolution, which causes a large amount of collateral vessels to remain undetected.[18,19] Nevertheless, microcirculation is the direct source of oxygen for the cardiac muscle cells and plays an indispensable role in regulating coronary flow and tissue perfusion quality.

It is commonly accepted that during ischemia an increased in vascular permeability, caused by continuous hypoxia injury, and an increased osmolality in the interstitial space attributed to catabolite accumulation are the preconditions for interstitial edema.[20,21] However, the source of the tissue fluid is still indeterminate when the blockage has not been cleared. It may originate from the adjoining capillary bed or from the collateral retrograde blood flow and leak out through the damaged original blood vessels. However, endothelial cells are extremely tolerant to hypoxia. Significant damage to the endothelial cell membrane structure and increased endothelial permeability are found notably later than the visible interstitial edema in AMI.[22,23] This is beyond the explanation of both hypotheses. Therefore, the description of the mechanism of myocardial interstitial edema put forward by traditional thinking remains to be further studied.

Essentially, the aim of this article is to (1) explore the performance of native collateral circulation and native collateral blood flow during the early stage of AMI in rats and (2) reveal the collateral microcirculation from the perspective of morphology and function.

Methods

The data that support the findings of this study are available from the corresponding author upon reasonable request.

All experiments were performed in adherence with the National Institutes of Health (NIH Publication, 8th Edition, 2011) guidelines on the use of laboratory animals. The animal care and experimental protocols were approved by the Xuzhou Medical University Committee on Animal Care, and studies on humans were approved by the Clinical Research Ethnics Committee of affiliated Hospital of Xuzhou Medical University (Jiangsu, China).

Animal Feeding and Treatment

Sprague-Dawley (SD) male rats (weighing approximately 250±10 g, at 8–10 weeks of age; n=206) were obtained from the Experimental Animal Center of Xuzhou Medical College. Rats were housed in a controlled environment (humidity, 50–60%). A total of 3 rats were housed per cage and were maintained at room temperature under a 12-hour light/dark cycle; rats were provided free access to food and water.

Enoxaparin was produced by Sanofi Winthrop Industrie (Floirac, France). SD rats were randomly divided into 3 groups: the control group, saline group, and enoxaparin group. The control group was only ligated with left anterior descending coronary artery (LAD). The saline group and the enoxaparin group received an intraperitoneal injection of saline (1 mL/kg) and enoxaparin (2 mg/kg) once a day for 3 days, respectively. After 8 to 12 hours of fasting, rats were used to build the AMI models.

Aspirin enteric-coated tablets were produced by Bayer Healthcare Limited Corporation (Leverkusen, Germany). SD rats were randomly divided into 3 groups: the control group, saline group, and aspirin group. The control group received normal feeding. Aspirin (300 mg/kg) and saline were administered by gavages, respectively, in the aspirin group and saline group, once a day for 3 days. After 8 to 12 hours of fasting, rats were used to build the AMI models.

Detailed grouping of each test can be found in Table.

Rat AMI Model

In order to shorten the time to close the thorax as much as possible, we have adopted a closed-chest rat model of

Table. Allocation of the Animals in the Groups

Methods	Groups	N	Comments	Figures
PET	Sham	8	Each rat was injected with 13N-NH3 3 times and scanned 3 times.	1B through 1D
	5 min			
	4 h			
Lectin-FITC perfusion and H&E stain (LAD)	Sham	6	One rat developed vessel injury and bleeding following passage of the needle through the LAD; lectin-labeled sections can be used for H&E staining without affecting H&E staining.	2A through 2D; 5C through 5E
	20 sec	6		
	5 min	9		
	30 min	6		
	1 h	6		
	2 h	6		
	4 h	9 (−1)		
	6 h	6		
Lectin-FITC perfusion and H&E stain (RCA)	Sham	6 (−1)	One rat died of cardiac arrest.	3A through 3D; 6A through 6E
	20 sec	6		
	5 min	6		
	30 min	6		
	1 h	6		
	2 h	6		
	4 h	6		
	6 h	6		
Lanthanum nitrate perfusion	Sham	5	Samples are not stained.	4A
	5 min	5		
Immunofluorescence (collagen IV/ZO-1/VE-cadherin)	Sham		Immunofluorescence was performed on sections labeled by lectin-FITC.	4B through 4E
	5 min			
TEM	Sham	9 (−1)	A rat died of anesthesia.	5F and 5G
	30 min	9		
Enoxaparin treatment	Sham	6	One rat died of ventricular fibrillation.	7A
	5 min	6 (−1)		
	4 h	7		
Aspirin treatment	Sham	6	One rat died of ventricular fibrillation.	7B
	5 min	6 (−1)		
	4 h	7		
Cardiac function	Sham	5		7C and 7D
	5 min	5		
	4 h	5		
Blood gas	Sham	5		7E through 7G
	5 min	5		
	4 h	5		

H&E indicates hematoxylin and eosin; LAD, left anterior descending coronary artery; PET, positron emission tomography; RCA, right coronary artery; TEM, transmission electron microscopy; VE-cadherin, vascular endothelial cadherin; ZO-1, zonula occludens-1.

myocardial ischemia designed by our team.[24] Related articles have been submitted to *Experimental and Therapeutic Medicine* (Y. Zhang et al, unpublished data, 2019). In brief, SD rats were anesthetized with sodium pentobarbital (60 mg/kg) intraperitoneally and maintained under anesthesia using isoflurane (1.5–2.0%) mixed with air. After adequate anesthesia, animals were intubated with a 14-gauge polyethylene catheter and the endotracheal tube was connected to a ventilator (Medical Equipment Company, Shanghai, China) with a rate of 250/min and a pressure of 4 to 6 cm H_2O. Placing rats in a supine position, left thoracotomy was performed through the fourth intercostal space under sterile condition. Following thoracotomy, a 6-0 prolene monofilament polypropylene suture (Ethicon, Somerville, NJ) was passed from below to loop the LAD. The 2 ends of the prolene suture were fixed to PE-10 tubes. Next, another 6-0 prolene suture was knotted along the loop. Then, a PE-10 tube was fixed to its end. Then, the pleural cavity was closed under positive end-expiratory pressure following the evacuation of air inside the chest. Then, a- and b-lines were tightened and the AMI models were completed under closed chest. The model was successfully established by ECG results. The completed model will be used for more operations, and the grouping will be specific to each experiment. This method also supports direct intramyocardial gene delivery.

Surface ECG Acquisition

ECG electrodes were attached to paws to obtain a baseline (PowerLab; AD Instruments, Colorado Springs, CO). Criteria for screening rats that could be included in the study were as follows: (1) no previous Q-wave; (2) no baseline ECG ST-segment abnormalities; and (3) no arrhythmia. Each rat's ECG was continuously monitored until the animal was culled.

Positron Emission Tomography

Positron emission tomography (PET) was performed by MITRO Biotech Co., Ltd. (Nanjing, China). The same animal was scanned 3 times by Micro PET (Siemens, Erlangen, Germany). The sham group's scan was performed the day before the AMI model was established. 13N-NH3 (300±150 μCi, half-life 10 minutes) was injected into rats through the tail vein before 3 scans, respectively. No abnormal reactions were observed in animals during this process. The closed-chest AMI models and PET imaging helped us to monitor the dynamic information of the native collateral blood flow.

Lectin-FITC Perfusion Experiment

One milliliter of 50 μg/mL of lectin from *Bandeiraea simplicifolia*/FITC (catalog no. L2895; Sigma-Aldrich, St. Louis, MO) was injected into the femoral vein of rat AMI models to mark blood vessels with perfusion in real time. After 30 seconds of blood circulation, hearts were harvested immediately for making frozen sections. Lectin-FITC follows the bloodstream to reach various grades of blood vessels, then nonspecifically binds glycoproteins on the surface of endothelial cells and marks them.

Lanthanum Nitrate Perfusion Experiment

Two percent lanthanum nitrate (catalog no. L812372; MACKLIN, Shanghai, China) dissolved in sodium dimethyl arsenate buffer. One to 2 mL of lanthanum nitrate solution was injected into the femoral vein of rat AMI models to mark blood vessels with perfusion in real time. After 30 seconds of blood circulation, hearts were harvested immediately for transmission electron microscope samples. Samples (1×1×1 mm) were taken from the infarct area.

Immunofluorescence

Sections were fixed for 15 minutes with 4% paraformaldehyde, permeabilized with Triton X-100 (0.1%), and blocked with solution containing 5% bovine serum before applying primary antibody.

Specimens were incubated, respectively, with anti-CD31 (catalog no. ab24590; 1:200; Abcam, Cambridge, MA); anti–prospero homeobox 1 (catalog no. 11067-2-AP; 1:100; ProteinTech Group Inc, Rosemont, IL); anti–vascular endothelial/cadherin (VE-cadherin; catalog no. ab33168; 1:300; Abcam); anti–zonula occludens-1 (ZO-1; (catalog no. 21773-l-AP; 1:100; ProteinTech Group); anti-ZO-1 (catalog no. 66452-1-lg; 1:100; ProteinTech Group); anti–collagen IV (catalog no. ab19808; 1:200; Abcam); and anti-fibroblast-specific factor1 (catalog no. S100A4; 1:200; Abcam) for 12 hours in 4°C. Secondary antibodies (catalog no. A21207; 1:200; Life Technologies, Carlsbad, CA) and Alexa Fluor 488 goat antimouse immunoglobulin G (catalog no. A11001; Life Technologies) were incubated subsequently under light-protected conditions for 1 hour at room temperature. Nuclei were stained with 4′,6-diamidino-2-phenylindole (catalog # KGA215–10; KeyGEN BioTECH Corp., Ltd, Nanjing, China) in the end. After final washing, coverslips were mounted on slides using 50% glycerin. Then, sections were observed under a fluorescence microscope (Olympus, Tokyo, Japan) or confocal laser scanning microscope (Olympus).

Vascular Density Measurement

Sections from hearts that had been injected by ectin from *Bandeiraea simplicifolia*/FITC were fixed in 4% paraformaldehyde for

15 minutes, washed 3 times in PBS, and covered with 50% glycerin in the end. Samples were scanned by the Slide Scanning System (Olympus VS120) to acquire panoramas. Ten randomly selected visual fields (15×) in infarct area for each sample and vessel density were measured. All quantitative evaluations were performed with ImagePro Plus software (Media Cybernetics, Rockville, MD).

Myocardial Interstitial Edema Area Measurement

Frozen sections were stained using hematoxylin and eosin in order to detect interstitial edema. Images were acquired using the Slide Scanning System (Olympus VS120). Translucent areas in sections are defined as myocardial interstitial edema area. Ten fields (20×) in the infarct zone and 10 fields (20×) in the relative normal area (the right ventricular wall for LAD ligation, the left ventricular wall for right coronary artery [RCA] ligation) were randomly selected for each sample and measured by an observer blinded to treatment group with ImagePro Plus software (Media Cybernetics).

Transmission Electron Microscopy Imaging and Analyses

Myocardial tissue treated with lanthanum nitrate were fixed with 2.5% glutaraldehyde overnight and then incubated in 1% osmium tetroxide for 2 hours with lightproof. After washing in distilled water, samples were incubated with 2% uranyl acetate for 2 hours at room temperature and then dehydrated in ethanol concentration gradient. The final step in making the samples is embedment with fresh resin. Ultrathin sections were cut with an EM UC7 (Leica Microsystems GmbH, Wetzlar, Germany) and examined with a Tecnai G2 T12 (FEI, Hillsboro, OR). In the process of shooting electron microscopy, lanthanum-nitrate–labeled microvessels are defined as vessels with perfusion in real time. On this basis, structural characteristics of coronary collateral microcirculation reserve (CCMR) and perivascular interstitial edema were observed.

Western Blotting Analysis

Primary antibodies for VE-cadherin, ZO-1, or Na^+/K^+-ATPase were followed by fluorescently labeled antimouse or -rabbit antibodies (LI-COR Biotechnology, Lincoln, NE) and imaged using the Odyssey infrared imaging system (LI-COR Biotechnology). Western blots were quantified using ImageJ software (National Institutes of Health, Bethesda, MD). Protein levels were calculated from the ratio of corresponding protein/Na^+/K^+-ATPase.

Cell Culture and Treatment

Rat primary cardiac microvascular endothelial cells (Cell Biologics Inc, Chicago IL) were used between the third and fifth passage and cultured in endothelial cell medium (catalog no. 1001; ScienCell Research Laboratories, Inc, Carlsbad, CA) supplemented with 5% FBS (catalog # 0025; ScienCell), 1% endothelial cell growth supplement (catalog # 1052; ScienCell), and 1% penicillin/streptomycin solution at 37°C in a humidified atmosphere containing 5% CO_2. The medium was replaced every 2 to 3 days, and cells were subcultured or subjected to experimental procedures at 80% to 90% confluence. Oxygen-glucose deprivation (OGD) was achieved by culturing cells in glucose-free DMEM (Gibco, Grand Island, NY) without FBS supplement for glucose deprivation and in a tri-gas incubator (Heal Force, Shanghai, China) saturated with 1% O_2/5% CO_2/94%N_2 at 37°C for 30 minutes, 1 hour, 2 hours, 4 hours, and 6 hours, respectively.

Permeability Measurement In Vitro

Permeability of monolayer rat primary cardiac microvascular endothelial cells were examined using cell-culture Transwell inserts (Transwell [12 mm diameter, 0.4 mm poresize]; Corning, Cambrige, MA). Cells were maintained at confluence on porous polyester membrance inserts before experimentation. Media (150 and 0.5 mL) were added into the upper and lower compartments. Then, 10 μmol/L of dextran-FITC was added to the upper chambers of the inserts. After hypoxia treatment, respectively, a 50-μL sample of medium was taken in triplicate from the lower chamber and placed in 96-well cluster plates (black with clear bottoms, polystyrene; Corning Costar; Corning) to measure fluorescence intensity (excitation at 530 nm and emission at 590 nm). The dextran-FITC that passed across the endothelial cell monolayer was normalized to the fluorescence reading from the upper chamber, and permeability was calculated as relative fluorescence units.

Determination of Cardiac Function

SD rats were anesthetized with sodium pentobarbital (60 mg/kg) intraperitoneally and maintained under anesthesia using isoflurane (1.5–2.0%) mixed with air. Blunt free right common carotid artery and a polyethylene Millar catheter was inserted into the right common carotid artery and then further advanced into the left ventricular chamber, and the cannula was connected to a pressure transducer. Proper positioning of the pressure sensor was verified by echocardiography. Mean arterial pressure and left ventricular end-diastolic pressure were recorded using an 8-channel polygraph system (PowerLab; AD Instruments).

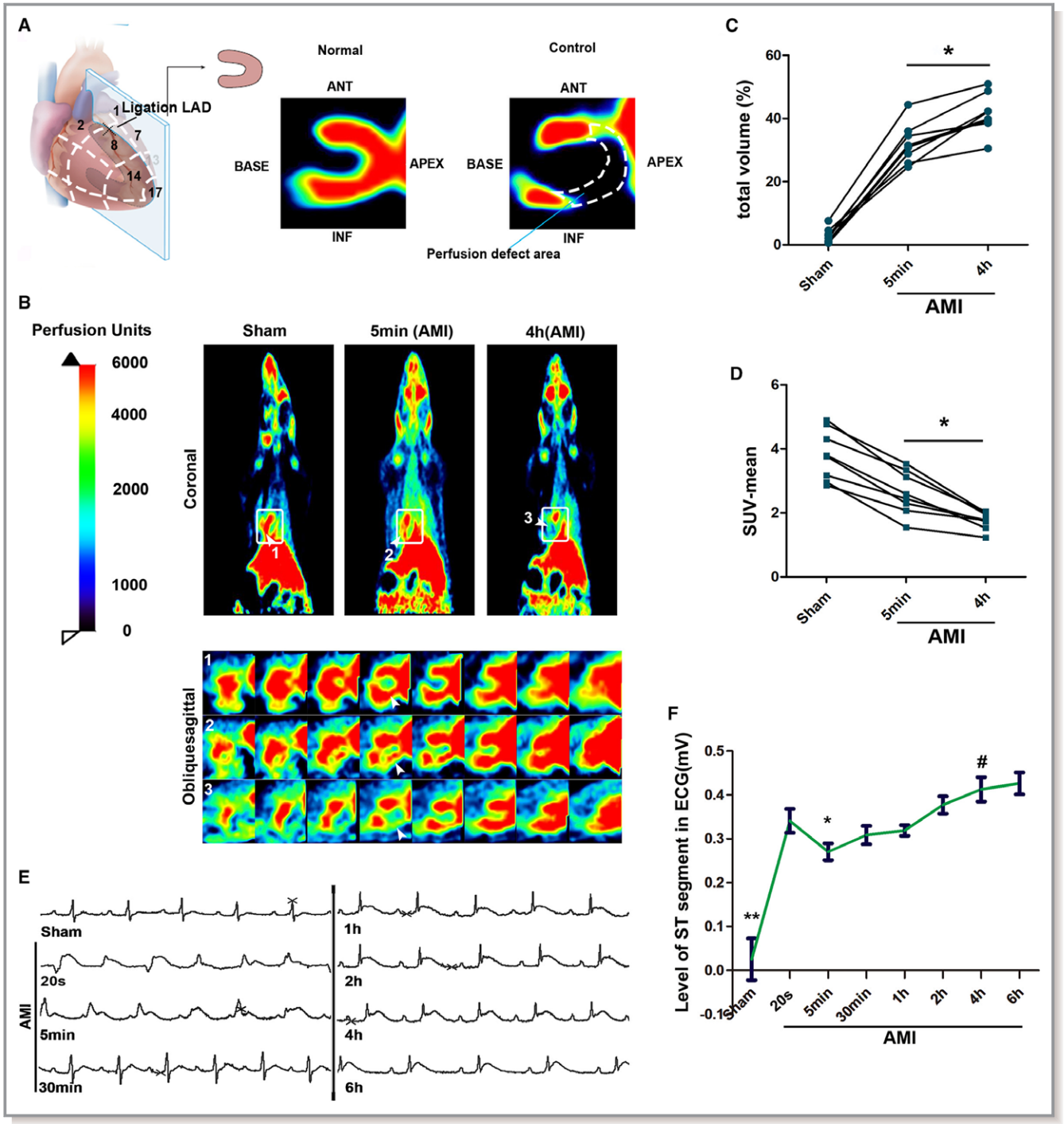

Figure 1. When the native collateral blood flow shows a recessive trend in the early time of acute myocardial infarction (AMI), it is considered a nonincident event. **A**, Schematic diagram of positron emission tomography (PET) perfusion imaging; tomographic images of cardiac perfusion defects area in rat hearts after blocking the left anterior descending coronary artery as shown in the figure. **B**, Representative images of perfusion (13N-NH3) by PET scan before ligation and 5 minutes and 4 hours after ligation in the same rat. The upper part is a representative coronal image of a systemic perfusion; the lower part is a continuous tomographic image in oblique sagittal corresponding to the rectangular frame (arrows indicate area of myocardial perfusion; n=8). **C**, Quantification of ischemic myocardial volume (*P<0.05 vs 5 minutes). **D**, Quantification of SUV mean of the hearts. *P<0.05 vs 5 minutes ischemic. SUV $= \frac{\text{uptake of radioactive substances in the region of interest}\,(\mu\text{Ci/g})}{\text{total injection dose}\,(\mu\text{Ci})/\text{weight}\,(\text{g})}$. **E**, Corresponding ECG. **F**, The representative ECG demonstrated a temporary fall of ST segment after AMI. *P<0.05 vs AMI 20 seconds; **P<0.01 vs AMI 20 seconds; $^{\#}P$<0.05 vs AMI 5 minutes (n=8). SUV indicates standard uptake value.

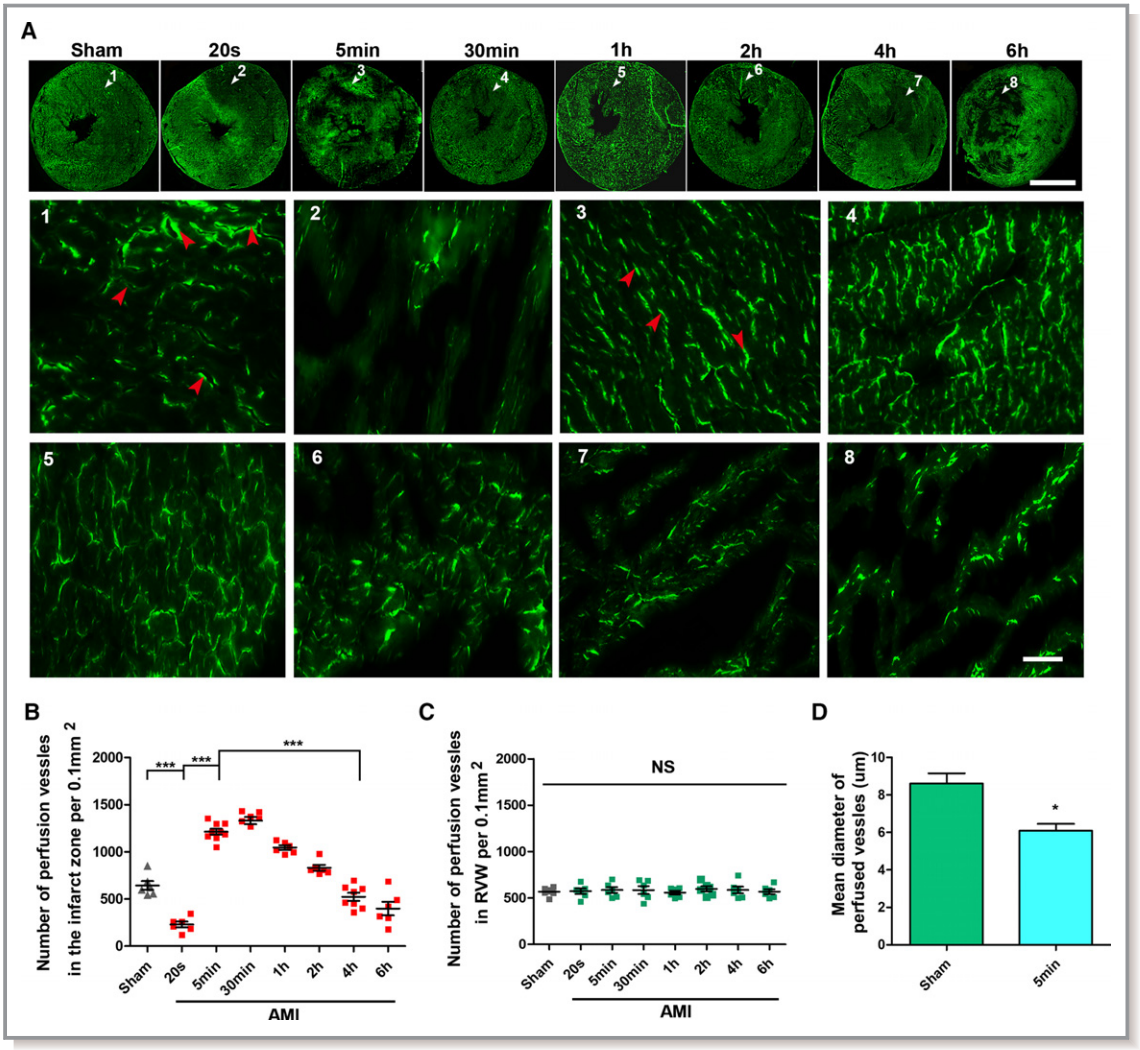

Figure 2. Distribution of CCMR vessels in rat hearts (the left ventricular myocardium). **A**, Lectin-FITC perfusion experiment was conducted in rats to mark vessels with blood perfusion at 20 seconds, 5 minutes, 30 minutes, 1 hour, 2 hours, 4 hours, and 6 hours ligation of the left anterior descending coronary artery; bar (upper)=5 mm, bar (lower)=50 μm. White arrows are the selected representative area; red arrows indicate perfused microvessels labeled by lectin-FITC (n=6–9). **B** and **C**, Quantification of vessels with blood perfusion in infarction zone (left ventricular wall) and relative normal region (right ventricular wall; RVW); values are means±SD; **P*<0.05 vs the sham group; ****P*<0.001 vs the indicated groups NS; *P*>0.05 vs the sham group. **D**, Quantification of mean diameter of perfused vessels in the sham and 5-minute group. **E**, Light microscopy analyses coexpression of CD31 (red) in lectin-labeled vessels (green) in 5-minute group cardiac sections (bar=50 μm; n=7). **F**, Light microscopy analyses coexpression of PROX1 (red) in lectin-labeled vessels (green) in 5-minute group cardiac sections (bar=50 μm). **G** and **H**, Quantification of $CD31^+$ $Lectin^+$ vessels and $PROX1^+Lectin^+$ vessels. CCMR indicates coronary collateral microcirculation reserve; NS, not significant; PROX1, prospero homeobox 1.

Blood Gas Analysis

Blood gas was measured at the exposed femoral arteries after rats were anesthetized. A sample (0.5 mL) of blood was taken with the Arterial Blood Gas Sampler (3302, 3cc; Westmed, Inc, Tucson, AZ) before ligation and 5 minutes and 4 hours after AMI, respectively. Samples were analyzed by an automatic blood gas system (GEM Premier 3500; Instrumentation Laboratory, Bedford, MA).

Statistical Analysis

Data are expressed as means±SEM. Multiple group comparisons were evaluated by 1-way ANOVA followed by least significant difference *t* test for post hoc analysis. Data between 2 independent groups were compared using a 2-tailed Student *t* test. Comparisons between repeated measurements, which were taken over time on the same rat, were performed using a paired Student *t* test. Analyses were performed using

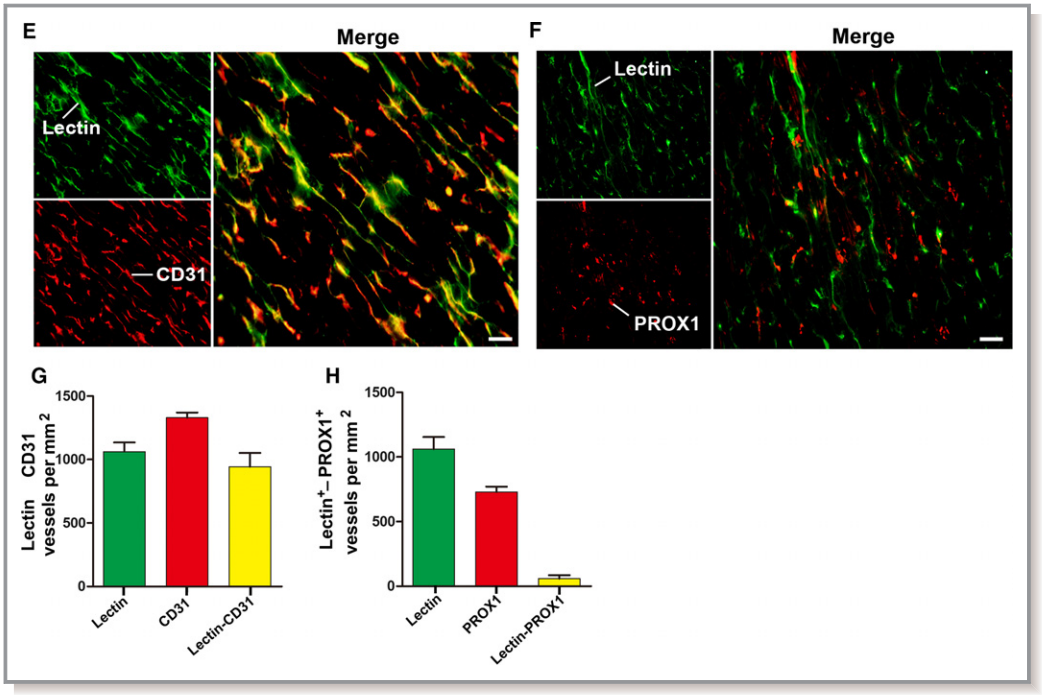

Figure 2. Continued

SPSS Software (SPSS, Inc, Chicago, IL). $P<0.05$ was considered as a significant difference.

Results

When the Native Collateral Blood Flow Shows a Recessive Trend in the Early Time of AMI, It Is Considered a Nonincident Event

In recent studies on coronary collateral circulation, we found that the time points for assessing collateral blood flow have been ambiguous. No study has indicated whether this will affect the accuracy of collateral function evaluation. Neutron-activated microspheres was a widely used experimental method for detecting collateral blood flow in these studies. However, measurement of collateral by microspheres (15 μm) was not accurate enough and did not allow the acquisition of data on changes of collateral functions after AMI. Therefore, PET perfusion imaging with 13N-NH3 was conducted before ligation, 5 minutes after ligation, and 4 hours after ligation in the same rat. A complete blockage of the LAD artery was ensured to block blood flow in the lower reaches of the ligation. A representative perfusion defect area tomogram when the LAD was completely blocked is shown in Figure 1A. Interestingly, an uneven low-intensity compensatory blood flow can be observed in the ischemic area at 5 minutes after ligation (Figure 1B). However, this native collateral blood flow is unstable. It will be reduced by 40% to 60% at 4 hours after blockage (Figure 1C and 1D), and this is a very critical phenomenon that has been ignored in the past. Significant elevation of the ST segment in the ECG suggested that accurate ligations had been performed. In addition, the ECG also showed a transient ST-segment depression during AMI (Figure 1E and 1F). Degree of ECG ST-segment elevation is generally related to myocardial ischemia degree, which indirectly proves the instability of the native collateral blood flow.

Distribution of the Native Coronary Collateral Microcirculation in Rat Hearts

To trace the origin of this compensatory blood flow, lectin-FITC was injected into the rat's circulatory system by the femoral vein to reach all vessels and mark them in real time (Figure 2A). Lectin$^+$ vessels can be treated as vessels with blood perfusion. The results indicated that the lectin$^+$ vessels were nearly invisible in the downstream area of the occlusion within 20 seconds after ligation, whereas in the 5-minute group, the density of lectin$^+$ vessels in the same area was more than doubled that of the sham group. This is obviously the result contributed by the native collateral circulation. These native collateral microvessels are not only large in number, but also smaller in diameter than normal ones (Figure 2D).

Not surprisingly, these vessels became dysfunctional with the prolonged blockage. Four hours after ligation, vessels with

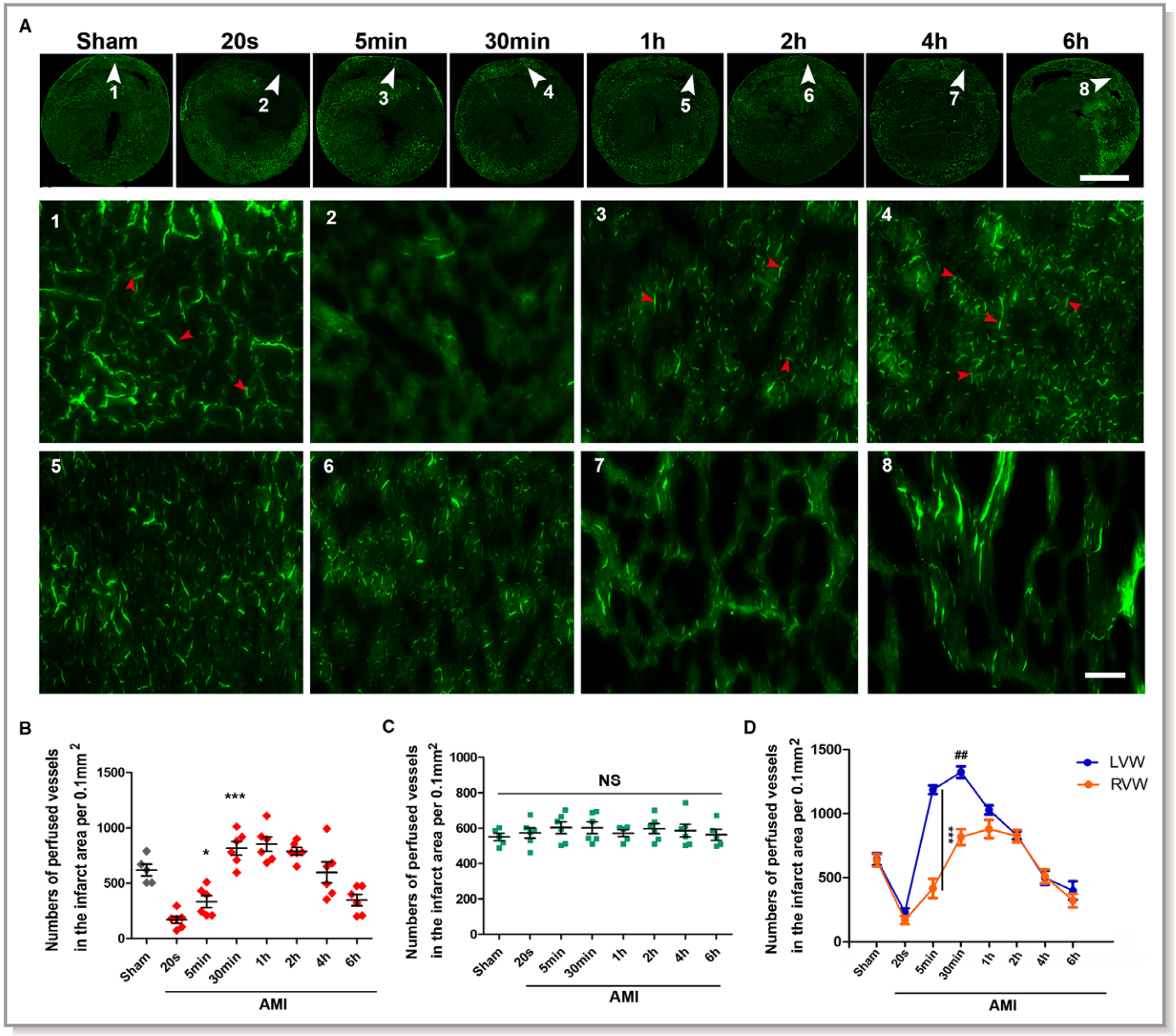

Figure 3. Inhomogeneous distribution of CCMR in rat hearts. **A**, Lectin-FITC perfusion experiment was conducted in rats to mark vessels with blood perfusion at 20 seconds, 5 minutes, 30 minutes, 1 hour, 2 hours, 4 hours, and 6 hours ligation of RCA (n=5–6); scale bar (upper)=5 mm; bar (lower)=50 μm. White arrows are the selected representative area; red arrows indicate perfused microvessels labeled by lectin-FITC. **B** and **C**, Quantification of vessels with blood perfusion in infarction zone (right ventricular wall; RVW) and relative normal region (left ventricular wall; LVW); values are means±SD; **P*<0.05 vs the 20-second group; ****P*<0.001 vs the sham group. D, Comparison of CCMR in LVW and RVW; ****P*<0.001 vs indicated group; $^{\#\#}$*P*<0.05 vs the 1-hour group (orange). AMI indicates acute myocardial infarction; CCMR, coronary collateral microcirculation reserve; NS, not significant; RCA, right coronary artery.

perfusion in the infarct zone rapidly decreased by ≈80% (Figure 2B). These results also explained why the compensatory blood flow presented by PET eventually disappeared. In addition, ligation of LAD did not affect blood vessels in the right ventricular myocardium (Figure 2C). Prospero homeobox 1 and CD31 immunofluorescence staining were conducted to identify whether blood vessels or lymphatic vessels were present (Figure 2E through 2H).

In brief, these native microcollateral (5–7 μm) bypasses in the rat heart serve as a blood flow reserve under physiological conditions, but temporarily recruit effective flow when AMI occurs. Therefore, we named them the CCMR. Distribution of CCMR in rat hearts is not homogeneous. We established the rat AMI models by ligating the right coronary artery to explore whether there is a similar distribution of CCMR in the right ventricular myocardium

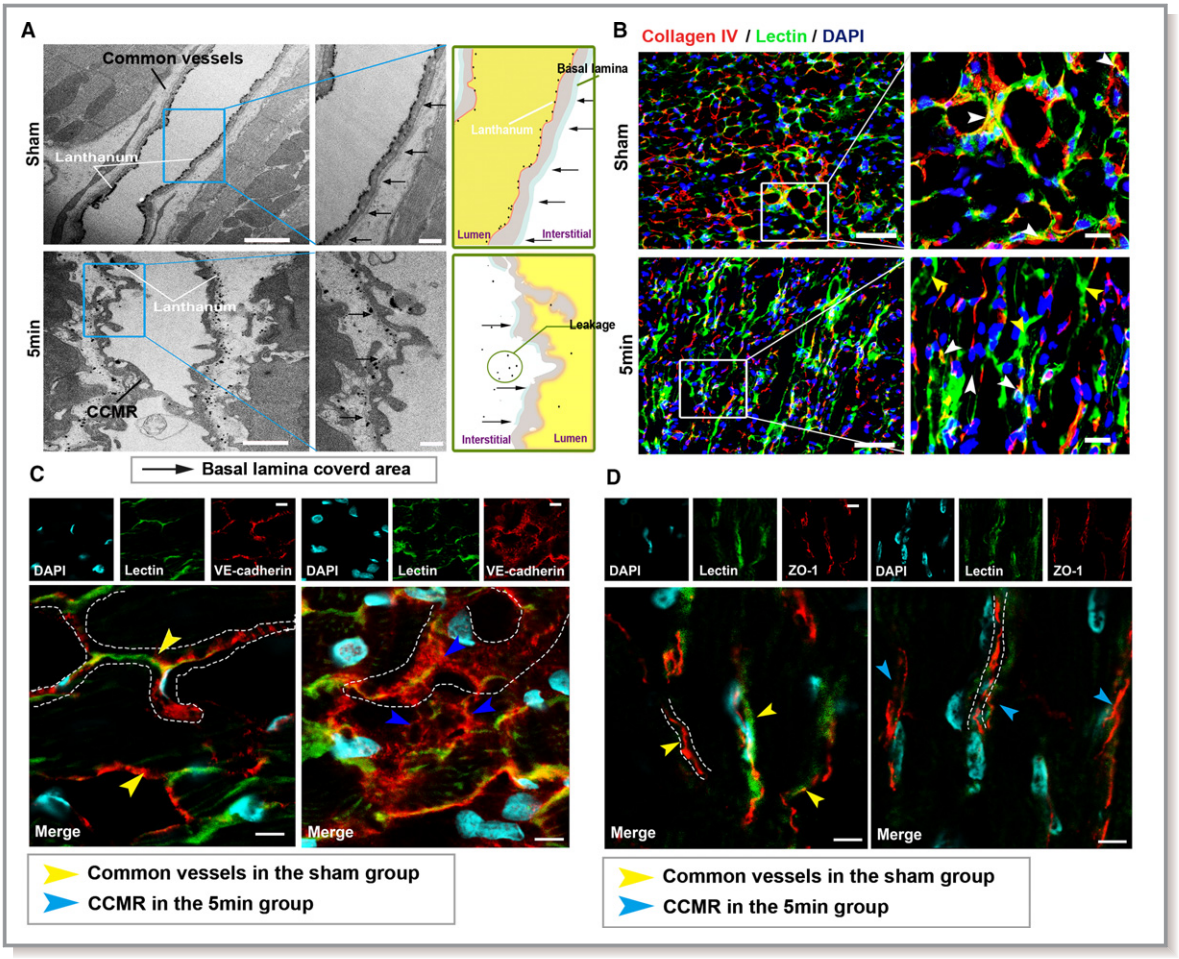

Figure 4. Defective structural characteristics of CCMR vessels. **A**, Left, transmission electron microscopy; black arrows indicate basal lamina area. Right, schematic of images on the left. **B**, Immunofluorescence images. Light microscopy analyses coexpression of collagen IV (red) in lectin-labeled (green) vessels in ischemic region of 5-minute group cardiac sections (CCMR) and the same region of the sham group (common vessels). White arrows indicate collagen IV coverage area of perfused vessels; yellow arrows indicate collagen IV deletion area of perfused vessels (n=9). **E**, Quantification of collagen IV coverage area of perfused vessels; values are means±SD; ***P<0.001 vs the sham group. **C** and **D**, Confocal immunoflourescence analysis of expression and distribution of VE-cadherin and ZO-1 in CCMR vessels. **F**, Western blot for VE-cadherin and ZO-1 on the endothelial cell membrane subjected to OGD (oxygen-glucose deprivation); **P<0.01; $^{\#\#}P$<0.01 vs the normal group (n=4). **G**, Immunofluorescence for VE-cadherin and ZO-1 on the endothelial cell membrane subjected to OGD. **H**, Transwell for permeability of the endothelial cell subjected to OGD; *P<0.05 vs the sham groups, NS; P>0.05 vs the sham group (n=4). Scale bars, 1 μm (A [left]), 500 nm (A [right]), 50 μm (B [left]), 20 μm (B [right]), and 10 μm (C, D, and G). CCMR indicates coronary collateral microcirculation reserve; DAPI, 4′,6-diamidino-2-phenylindole; NS, not significant; VE-cadherin, vascular endothelial cadherin; ZO-1, zonula occludens-1.

(Figure 3A). Results showed that the density of CCMR in the right ventricle myocardium is milder than that in the left ventricular myocardium. Moreover, we also found that ischemia induces the activation of CCMR in the left ventricle myocardium notably earlier than that in the right ventricle myocardium (Figure 3B through 3D).

Morphological and Structural Features of CCMR Vessels

Structural integrity of vessels is a precondition of stable vascular perfusion. To study the structural features of the CCMR, the priority was to distinguish them from the functional circulatory system under physiological conditions in the microscopic perspective. Lanthanum nitrate (sized 1–4 nm) and lectin-FITC were injected into femoral vein as markers for blood flow. Respectively, lanthanum$^+$ or lectin$^+$ vessels in sham-operated rats were treated as the common vessels, and lanthanum$^+$ or lectin$^+$ vessels in the ischemic area in the 5-minute group are defined as CCMR. Undyed samples were observed by electron microscope (Figure 4A). In the sham group, continuous basement membrane could be found in common vessels, and lanthanum nitrate was completely confined within the lumens. In the infarct zone of

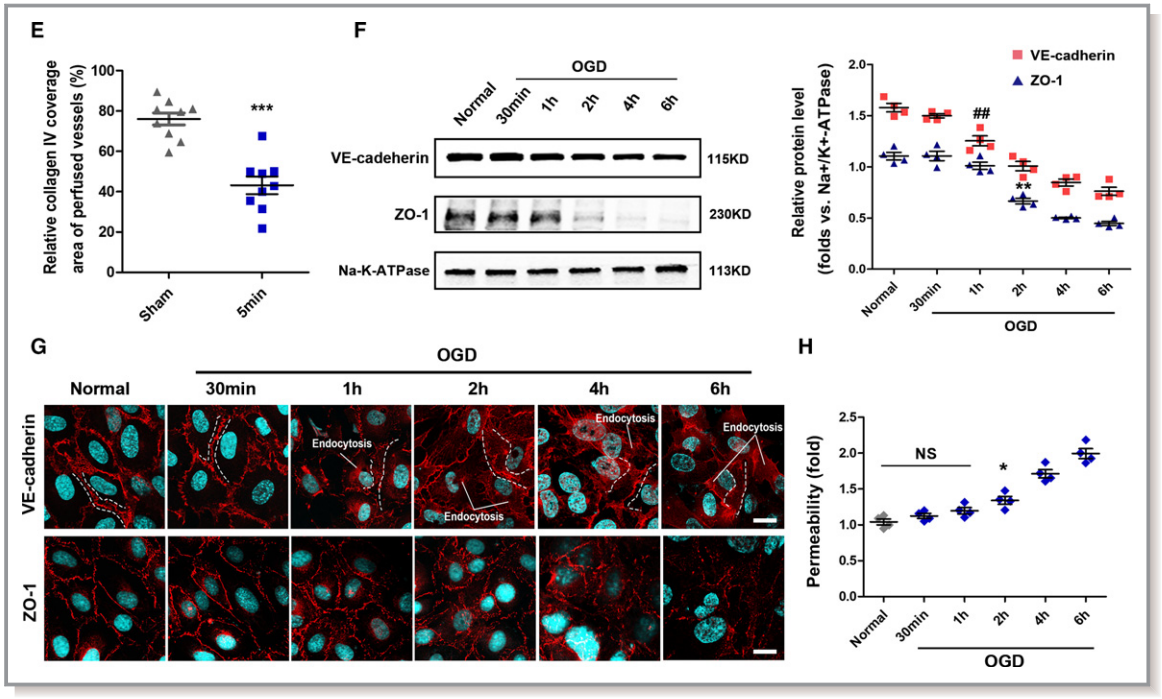

Figure 4. Continued

the 5-minute group, the CCMR vessels exhibited lanthanum^{+}. The basement membrane of CCMR vessels is discontinuous. Lanthanum nitrate leaked out of CCMR vessels and was deposited in the interstitial area. To further understand the structural features of CCMR, VE-cadherin, ZO-1, and collagen IV were stained in sections of sham groups and 5-minute groups that were labeled with lectin-FITC. Collagen IV coverage of CCMR vessels was only approximately half of that in common vessels (Figure 4B and 4E). Immunofluorescence analysis also showed a loose distribution of VE-cadherin, which is the most important adhesion junction structural protein in CCMR (Figure 4C). However, compared with common vessels, there was no significant difference in expression and distribution of ZO-1, an important tight junction structural protein (Figure 4D).

Characteristics of the VE-cadherin protein in CCMR endothelial cells are similar to those of endothelial cells treated with OGD, in which condition, VE-cadherin detaches from the membrane and enters the cytoplasm by endocytosis. It is obvious that the defective structures of CCMR were not caused by 5 minutes of ischemia. We demonstrated this conclusion again in vitro. First, we tested expression of VE-cadherin and ZO-1 on OGD-treated rat cardiac microvascular endothelial cells. Level of VE-cadherin on the membrane was significantly decreased at OGD 2 hours. A similar performance of ZO-1 occurred at OGD 4 hours (Figure 4F). Furthermore, immunofluorescence assay revealed similar results. ODG treatment for ≈2 hours induced VE-cadherin endocytosis. VE-cadherin transferred from membrane to cytoplasm and expressed as a loose distribution on the membrane (Figure 4G). In transwell experiment, permeability of the endothelial cell increased significantly subjected to OGD 2 hours (Figure 4H). Obviously, it is unlikely that these vascular lesions secondary to hypoxia will occur within 5 minutes of blocking blood flow to the LAD. These results suggest that structures of CCMR vessels were natively defective, leading to a greater permeability and deteriorated function.

Opening of CCMR Vessels Leads to Vascular Leakage and Interstitial Edema

We further detected the exudation of fibrinogen in the ischemic area, and a small amount of fibrinogen could be detected outside the blood vessel 5 minutes after infarction, which developed into a gradually accelerating trend in the subsequent process (Figure 5A and 5B). Then, we examined the trend of the occurrence of interstitial edema after AMI by hematoxylin and eosin staining (Figure 5C). Results indicated that significant interstitial edema occurred 30 minutes after infarction, surged for 1 hour, and approached saturation 4 hours later (Figure 5D). In addition, interstitial edema was always initiated in the infarction area and diffused around it as the center. The interstice of the region located away from the infarction zone was also affected within AMI (Figure 5E). Notable interstitial edema between capillaries and myocardium could be detected by transmission electron microscope in the infarction region 30 minutes after AMI (Figure 5F and

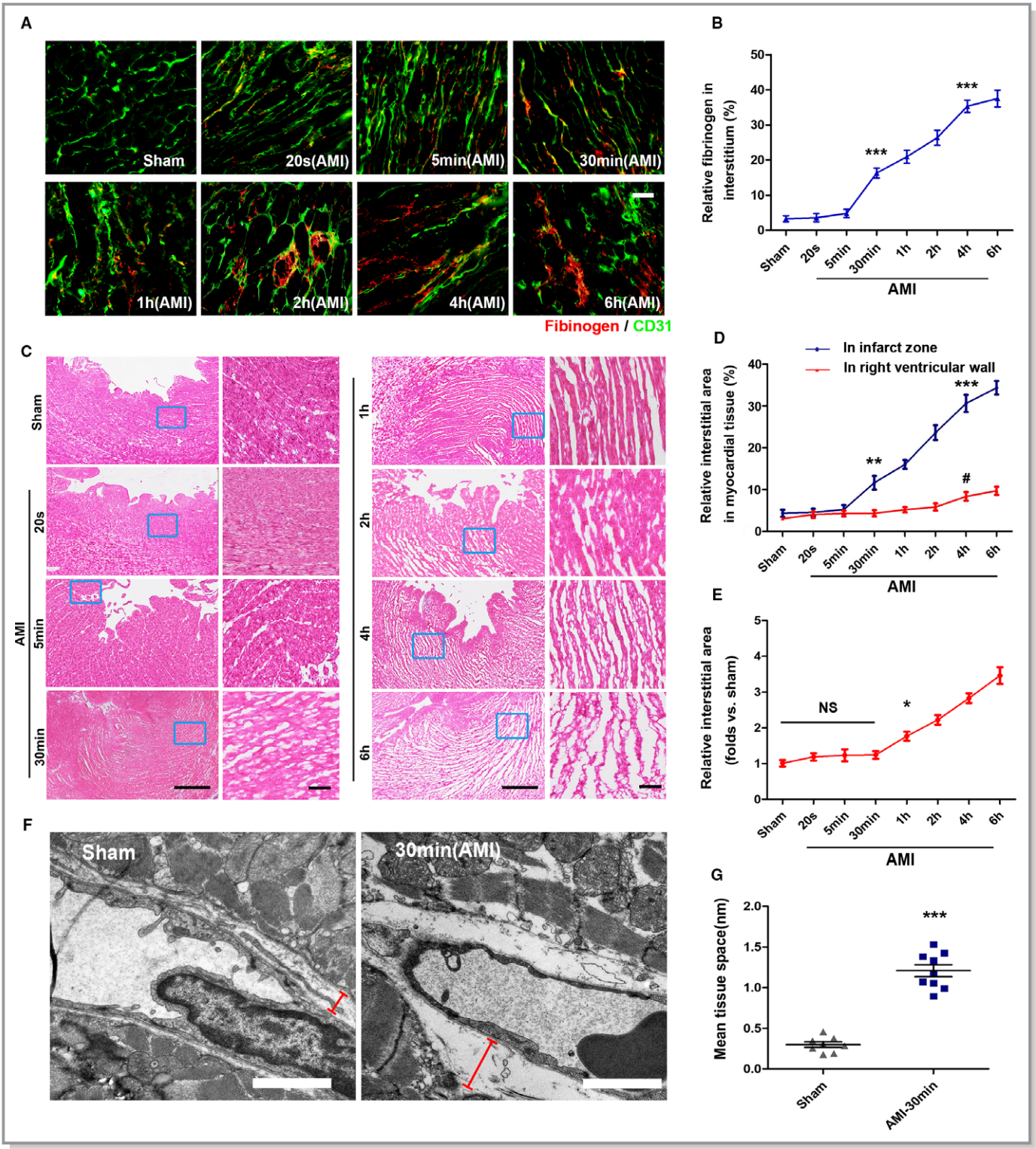

Figure 5. Openings of CCMR vessels lead to vascular leakage and interstitial edema. **A** and **B**, Exudation of fibrinogen in blood was detected by immunofluorescence; ***P<0.001 vs the sham group (n=7). **C**, Heart sections stained with H&E (n=6–9). **D**, Quantification of interstitial area in the infract area and relative normal region (right ventricular wall); **P<0.01 vs the sham group (blue); ***P<0.001 vs the sham group (blue); $^{\#}P$<0 .05 vs the sham group (red). **E**, Quantification of interstitial area in relative normal region (right ventricular wall); *P<0.05 vs the sham group, NS; P>0.05 vs the sham group. **F** and **G**, Transmission electron microscopy (red signs indicate the interstitial region) and tissue space statistics. ***P<0.001 vs the sham group (n=8–9). Scale bars, 50 μm (A), 1 mm (C [left]), 50 μm (C [right]), 1 μm (F). AMI indicates acute myocardial infarction; CCMR, coronary collateral microcirculation reserve; H&E, hematoxylin and eosin; NS, not significant.

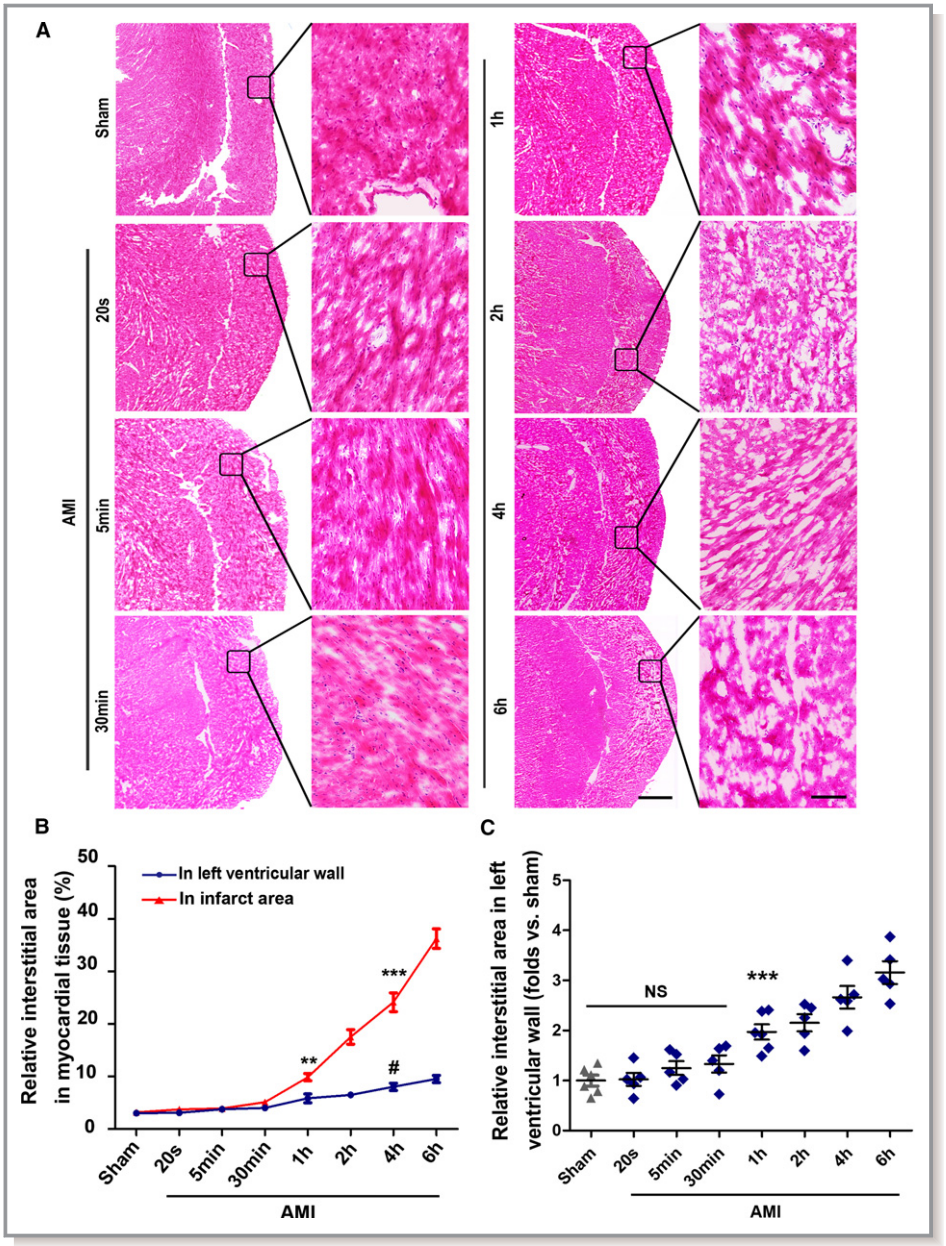

Figure 6. Interstitial edema in the early stage of RCA ligation. **A**, Heart sections from stained with H&E; scale bar (left)=1 mm; scale bar (right)=50 μm (n=5–6). **B**, Quantification of interstitial area in the infract area and relative normal region (left ventricular wall; LVW); $^{**}P<0.01$ vs the sham group (red); $^{***}P<0.001$ vs the sham group (red); $^{\#}P<0.05$ vs the sham group (blue). **C**, Quantification of interstitial area in relative normal region (LVW); $^{***}P<0.001$ vs the sham group, NS; $P>0.05$ vs the sham group. **D**, Comparison of interstitial edema in the infarct area between the ligation of LAD and RCA; $^{*}P<0.05$ vs the indicated group. **E**, A correlation analysis on the relationship between degree of interstitial edema and function of CCMR in the right ventricular wall (right ventricular wall). AMI indicates acute myocardial infarction; CCMR, coronary collateral microcirculation reserve; H&E, hematoxylin and eosin; LAD, left anterior descending coronary artery; NS, not significant; RCA, right coronary artery.

5G). Therefore, we hypothesized that the relatively abundant native collateral blood flow carried by CCMR in the infarct zone provides a source of water for interstitial edema in the early stage of AMI. The collateral blood flow is in the infarcted area, and the interstitial edema is centered on the infarcted area. The CCMR vascular structure is naturally immature, and interstitial edema occurs earlier than ischemia-induced vascular injury.

Interstitial edema in the right ventricle after ligation of the RCA was also detected (Figure 6A). Results indicated that blocking the RCA triggers severe interstitial edema in the right ventricle and affects the left heart (Figure 6B and 6C). Additionally,

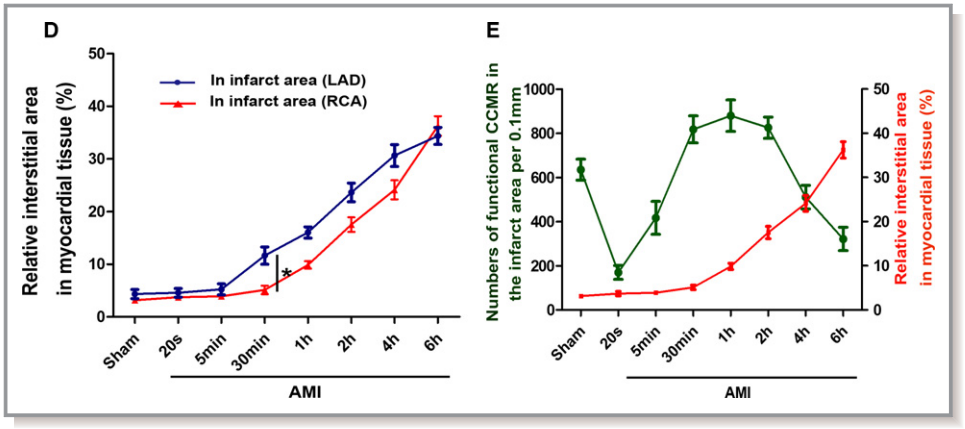

Figure 6. Continued

interstitial edema in the right ventricle occurs significantly later than in the left ventricle after AMI (Figure 6D). Next, we analyzed the relationship between degree of interstitial edema and the function of CCMR, and the results showed a reverse pattern when interstitial edema begins to occur (Figure 6E).

Possible Causes of Severe Recession of the Native Collateral Blood Flow

The common factors of vascular occlusion can be divided into internal blockage (embolization) and external force compression (tissue and interstitial edema).[25–27] During the experimental process, no extensive microemboli were observed under either the optical microscope or the electron microscope that resulted in blockage of the vascular lumen. Furthermore, we tested whether thrombogenesis is associated with dysfunction of CCMR. Rats were then treated with anticoagulant low-molecular-weight heparin and aspirin, which inhibits platelet aggregation. There was little effect on the function of CCMR in AMI rats after use of the 2 drugs (Figure 7A and 7B). Methods of anesthesia and surgery may also cause changes in arterial blood and blood gas, which may lead to instability of collateral flow. Therefore, we also monitored arterial pressure and blood gas before and during surgery. The results showed a decrease in mean arterial pressure after ligation of LAD. However, data of 5 minutes and 4 hours did not show significant changes or statistically trends. Results of left ventricular end-diastolic pressure showed similar results (Figure 7C and 7D). Therefore, we believe that arterial blood pressure is not the main cause of the decrease of native collateral blood flow in the early stage of AMI, although it is not clear whether arterial blood pressure would contribute to collaterals function. During and after the operation, we used mechanical ventilation (a rate of 250 pbm and a pressure of 4–6 cm H_2O) to support respiration of rats, and this very effectively limited the variety of blood gases/pH. Results show that only the partial pressure of carbon dioxide was slightly increased (Figure 7E through 7G).

Additionally, structural defects of CCMR vessels led to myocardial interstitial edema in the early stage of AMI. Continuous expansion of the interstitial edema gradually compressed vessels. Because of its immature structure, CCMR would receive a more-serious impact. We captured a large number of images as evidence of microvascular closure caused by severe interstitial edema compression (Figure 7H). Next, we analyzed the relationship between degree of interstitial edema and function of CCMR, and the results showed a reverse pattern when interstitial edema began to occur (Figures 7I and 6E). Taking into account these results, we speculated that the continuous expansion of the interstitial area will press the vessels and, in turn, disable CCMR.

Discussion

The aims of this article are to let readers further recognize the native coronary collateral blood flow and provide a preview of a distinctive collateral vascular system in the rat heart (ie, the CCMR).

As natural bypasses, native coronary collaterals provide an alternative source of blood flow to a myocardial area when AMI occurs. Contrary to popular belief, the blood flow deliverable by native collaterals can be sizeable and able to effectively support the ischemic myocardium before achieving recanalization.[13,28] In addition, alterations in blood flow and blood pressure promote shear and remodeling of native collaterals, which will further increase compensatory blood flow.[29–31]

The working mode of these collateral vessels under physio- and pathological conditions determines their roles as a blood flow reserve, even though the compensatory flow

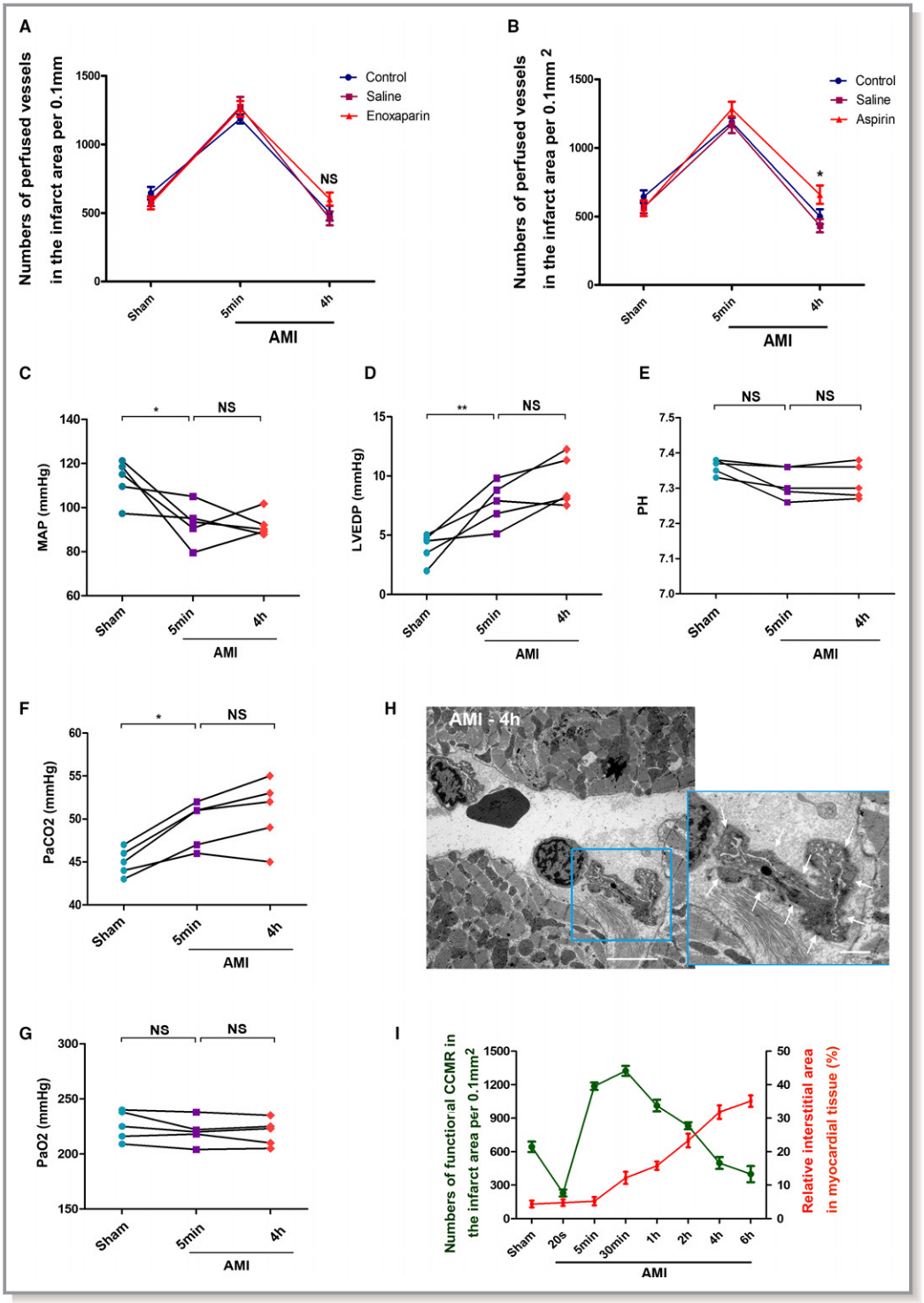

Figure 7. Possible causes of severe recession of the native collateral blood flow. A, Enoxaparin treatment, NS; $P>0.05$ vs the control group (n=5–7). B, Aspirin treatment; *$P<0.05$ vs the control group (n=5–7). C, Mean arterial pressure (n=5). D, Left ventricular end diastolic pressure; data are expressed as the means±SEM. *$P<0.05$; **$P<0.01$, NS; $P>0.05$ vs the indicated groups (n=5). E, pH value. F, Partial pressure of carbon dioxide ($PaCO_2$). G,PaO_2, *$P<0.05$, NS; $P>0.05$ vs the indicated groups (n=5). H, TEM for myocardial tissue in the infarct area (AMI 4 hours); white arrows indicate the pressure of interstitial edema on blood vessels. I, A correlation analysis on the relationship between degree of interstitial edema and function of CCMR in the left ventricular wall; bar (left)=5 μm; bar (right)=1 μm. AMI indicates acute myocardial infarction; CCMR, coronary collateral microcirculation reserve; NS, not significant.

they provide is only temporary. Distribution of CCMR suggests that the collateral circulation has independent microcirculation components similar to a conventional circulatory system. This indicates that compensatory blood flow can temporarily support the myocardium directly through CCMR. Although these collateral vessels have smaller diameters, the huge total cross-sectional area determines that the antegrade native collateral blood flow they can recruit is relatively abundant.

In this study, we first found that the native coronary collateral blood flow is extremely unstable in the early stage. We believe that this finding cannot be ignored in the studies on the distribution of collateral circulation, the native collateral blood flow intensity, and collateral function in animal models. Many research teams have made outstanding contributions to native collateral coronary circulation and the factors that stimulate the growth of coronary collaterals, such as the Chilian and Rocic groups. All their achievements, combined with our findings, will lead to a more-meaningful conclusion.

Schaper et al[28] postulate that collateral vessels are immature. After shearing and remodeling under the action of blood flow stress, only a few of them will eventually evolve into a mature state.[28,32] Our research shows that CCMR was with anatomical defects. A fragmentary basement layer and defects in adhesion junctions led to greater permeability of CCMR compared with common vessels. From this point of view, CCMR is also an immature blood vessel in structure and function. Therefore, once CCMR opens up to increase compensated blood flow, plasma exudation will follow. In addition, CCMR, which works in infarction areas, also provides a source of tissue fluid for production of interstitial edema. Thus, it provides a more-reasonable explanation for the severe interstitial edema in the early stage of AMI.

There is no denial that structural defects stop CCMR from continuously and steadily contributing to the native collateral blood supply. Our study indicated that interstitial edema is closely related to the function of CCMR. Evidence shows that the continuous expansion of the interstitial area will, in turn, press the vessels and disable CCMR.

Native collateral blood flow often originates from the adjacent coronary artery branches or upstream branches of blockages. We distinguished CCMR from common vessels in ischemic areas by blocking the LAD or RCA in real time, but were unable to identify the origin of CCMR in this area using this method. We recognize the importance of this issue and look to address it accordingly.

Despite the fact that the CCMR works as an alternative source of blood supply to a myocardial area jeopardized by ischemia, its transitory characteristics make it incapable of reversing the outcome of AMI. Therefore, if there was a similar distribution of CCMR in humans, conducting a study on the mechanism that causes the natural defects in CCMR structures, exploring the intervention-mediated remodeling that can overcome their structural defects, enhancing the compensatory blood supply to ischemic myocardium, relieving the poor prognosis caused by interstitial edema, and eventually improving heart performance will be a novel and promising strategy toward ischemic heart disease treatment in theory.

Acknowledgments

We thank Meng Wang (Morphological Research Experiment Center, Xuzhou Medical University) for TEM.

Sources of Funding

This work was supported by the grant from National Nature Science Foundation of China (81570242 and 81270173).

Disclosures

The authors disclose no conflict of interest.

References

1. Traupe T, Gloekler S, de Marchi SF, Werner GS, Seiler C. Assessment of the human coronary collateral circulation. *Circulation*. 2010;122:1210–1220.
2. Fujita M, Sasayama S. Reappraisal of functional importance of coronary collateral circulation. *Cardiology*. 2010;117:246–252.
3. Seiler C. The human coronary collateral circulation. *Eur J Clin Invest*. 2010;40:465–476.
4. Abbott JD, Choi EJ, Selzer F, Srinivas VS, Williams DO; National Heart, Lung, and Blood Institute Dynamic Registry. Impact of coronary collaterals on outcome following percutaneous coronary intervention (from the National Heart, Lung, and Blood Institute Dynamic Registry). *Am J Cardiol*. 2005;96:676–680.
5. Seiler C. Assessment and impact of the human coronary collateral circulation on myocardial ischemia and outcome. *Circ Cardiovasc Interv*. 2013;6:719–728.
6. Seiler C, Stoller M, Pitt B, Meier P. The human coronary collateral circulation: development and clinical importance. *Eur Heart J*. 2013;34:2674–2682.
7. Seiler C, Engler R, Berner L, Stoller M, Meier P, Steck H, Traupe T. Prognostic relevance of coronary collateral function: confounded or causal relationship? *Heart*. 2013;99:1408–1414.
8. Seiler C, Meier P. Historical aspects and relevance of the human coronary collateral circulation. *Curr Cardiol Rev*. 2014;10:2–16.
9. Valuckiene Z, Budrys P, Jurkevicius R. Predicting ischemic mitral regurgitation in patients with acute ST-elevation myocardial infarction: does time to reperfusion really matter and what is the role of collateral circulation? *Int J Cardiol*. 2016;203:667–671.
10. Faber JE, Chilian WM, Deindl E, van Royen N, Simons M. A brief etymology of the collateral circulation. *Arterioscler Thromb Vasc Biol*. 2014;34:1854–1859.
11. Lohr NL. Collateral development: the quest continues. *Circ Res*. 2014;114:591–593.
12. Toriumi H, Tatarishvili J, Tomita M, Tomita Y, Unekawa M, Suzuki N. Dually supplied T-junctions in arteriolo-arteriolar anastomosis in mice: key to local hemodynamic homeostasis in normal and ischemic states? *Stroke*. 2009;40:3378–3383.
13. Stoller M, Seiler C. Salient features of the coronary collateral circulation and its clinical relevance. *Swiss Med Wkly*. 2015;145:w14154.
14. Elias J, Hoebers LPC, van Dongen IM, Claessen B, Henriques JP. Impact of collateral circulation on survival in ST-segment elevation myocardial infarction

patients undergoing primary percutaneous coronary intervention with a concomitant chronic total occlusion. *JACC Cardiovasc Interv*. 2017;10:906–914.

15. Joseph G, Soler A, Hutcheson R, Hunter I, Bradford C, Hutcheson B, Gotlinger KH, Jiang H, Falck JR, Proctor S, Schwartzman ML, Rocic P. Elevated 20-HETE impairs coronary collateral growth in metabolic syndrome via endothelial dysfunction. *Am J Physiol Heart Circ Physiol*. 2017;312:H528–H540.
16. Carrao AC, Chilian WM, Yun J, Kolz C, Rocic P, Lehmann K, van den Wijngaard JP, van Horssen P, Spaan JA, Ohanyan V, Pung YF, Buschmann I. Stimulation of coronary collateral growth by granulocyte stimulating factor: role of reactive oxygen species. *Arterioscler Thromb Vasc Biol*. 2009;29:1817–1822.
17. Jadhav R, Dodd T, Smith E, Bailey E, Delucia AL, Russell JC, Madison R, Potter B, Walsh K, Jo H, Rocic P. Angiotensin type I receptor blockade in conjunction with enhanced Akt activation restores coronary collateral growth in the metabolic syndrome. *Am J Physiol Heart Circ Physiol*. 2011;300:H1938–H1949.
18. Rentrop KP, Cohen M, Blanke H, Phillips RA. Changes in collateral channel filling immediately after controlled coronary artery occlusion by an angioplasty balloon in human subjects. *J Am Coll Cardiol*. 1985;5:587–592.
19. Fulton WF. Arterial anastomoses in the coronary circulation. I. Anatomical features in normal and diseased hearts demonstrated by stereoarteriography. *Scott Med J*. 1963;8:420–434.
20. Friedrich MG. Myocardial edema—a new clinical entity? *Nat Rev Cardiol*. 2010;7:292–296.
21. Hoda SA, Cheng E. Robbins basic pathology. *Am J Clin Pathol*. 2017 Nov 6. doi: 10.1093/ajcp/aqx095. [Epub ahead of print].
22. Kloner RA, Rude RE, Carlson N, Maroko PR, DeBoer LW, Braunwald E. Ultrastructural evidence of microvascular damage and myocardial cell injury after coronary artery occlusion: which comes first? *Circulation*. 1980;62:945–952.
23. Kloner RA. The importance of no-reflow/microvascular obstruction in the STEMI patient. *Eur Heart J*. 2017;38:3511–3513.
24. Zhao Q, Liu Z, Huang B, Yuan Y, Liu X, Zhang H, Qiu F, Zhang Y, Li Y, Miao H, Dong H, Zhang Z. PEDF improves cardiac function in rats subjected to myocardial ischemia/reperfusion injury by inhibiting ROS generation via PEDF-R. *Int J Mol Med*. 2018;41:3243–3252.
25. Niccoli G, Burzotta F, Galiuto L, Crea F. Myocardial no-reflow in humans. *J Am Coll Cardiol*. 2009;54:281–292.
26. Diaz RJ, Armstrong SC, Batthish M, Backx PH, Ganote CE, Wilson GJ. Enhanced cell volume regulation: a key protective mechanism of ischemic preconditioning in rabbit ventricular myocytes. *J Mol Cell Cardiol*. 2003;35:45–58.
27. Jackson SP. Arterial thrombosis—insidious, unpredictable and deadly. *Nat Med*. 2011;17:1423–1436.
28. Schaper W. Collateral circulation: past and present. *Basic Res Cardiol*. 2009;104:5–21.
29. Gould KL. Pressure-flow characteristics of coronary stenoses in unsedated dogs at rest and during coronary vasodilation. *Circ Res*. 1978;43:242–253.
30. Carmeliet P. Mechanisms of angiogenesis and arteriogenesis. *Nat Med*. 2000;6:389–395.
31. Schaper W, Scholz D. Factors regulating arteriogenesis. *Arterioscler Thromb Vasc Biol*. 2003;23:1143–1151.
32. Meier P, Seiler C. The coronary collateral circulation—past, present and future. *Curr Cardiol Rev*. 2014;10:1.